Detectable inertial effects on Brownian transport through narrow pores

Pulak Kumar Ghosh[1,2], Peter Hänggi[2], Fabio Marchesoni[3], Franco Nori[1,4] and Gerhard Schmid[2]

[1] *Advanced Science Institute, RIKEN - Wako-shi, Saitama, 351-0198, Japan*
[2] *Institut für Physik, Universität Augsburg - D-86135 Augsburg, Germany*
[3] *Dipartimento di Fisica, Università di Camerino - I-62032 Camerino, Italy*
[4] *Physics Department, University of Michigan - Ann Arbor, MI 48109, USA*

Brownian transport in narrow corrugated channels is a topic of potential applications to both natural [1,2] and artificial devices [3]. Depending on the amplitude and geometry of the wall modulation, corrugated channels fall within two distinct categories: i) smoothly corrugated channels, typically modeled as quasi–one-dimensional (1D) periodic channels with axial symmetry and unit cells delimited by smooth, narrow bottlenecks, also called pores [4–12]; ii) compartmentalized channels [13–16], formed by identical compartments separated by thin dividing walls and connected by narrow pores centered around the channel axis. Brownian transport in such sharply corrugated channels must be treated as an irreducible two- or three-dimensional diffusion problem [17]. More importantly, for both categories of corrugated channels most analytical results only apply under the condition of very narrow pores [2,5,17].

Corrugated channels are often used to model transport of dilute mixtures of small particles (*e.g.*, biomolecules, colloids or magnetic vortices) in confined geometries [3]. Each particle is subjected to thermal fluctuations with temperature T and large viscous damping γ, and a homogeneous constant bias of strength F parallel to the channel axis. Such a dc drive is applied by coupling the particle to an external field (*e.g.*, by attaching a dielectric or magnetic dipole, or a magnetic flux to the particle), without inducing drag effects on the suspension fluid. Interparticle and hydrodynamic interactions are thus ignored for simplicity (these assumptions are discussed in ref. [4]).

In this paper we investigate the relevance of inertial effects due to the viscosity of the suspended particle. As is often the case with biological (and most artificial) suspensions [3], the Brownian particle dynamics in the bulk can be regarded as overdamped. This corresponds to i) formally setting the mass of the particle to zero, $m = 0$, or, equivalently, to making the friction strength γ tend to infinity, and ii) assuming F smaller than the thermal force $F_0 = \gamma\sqrt{kT/m}$ (Smoluchowski approximation) [18]. The current literature on corrugated channels invariably assumes such an overdamped limit. But how large is an "infinite" γ (or how small can be a "zero" m)? The answer, of course, depends on the geometry of the channel. Our main conclusion is that the overdamped dynamics assumption for Brownian diffusion through pores of width Δ subjected to a homogeneous drive F, applies only for $\gamma \gg \sqrt{mkT}/\Delta$ and $\gamma \gg \sqrt{mF/\Delta}$, irrespective of the degree of corrugation. This means that the inertial effects cannot be neglected as long as the Brownian diffusion is spatially correlated on a length ($l_T = \sqrt{mkT}/\gamma$ at small dc drive, or $l_F = mF/\gamma^2$ at large dc drive) of the order of, or larger than, the pore width Δ. Therefore, for sufficiently narrow pores or sufficiently large drives, inertia always comes into play by enhancing the blocking

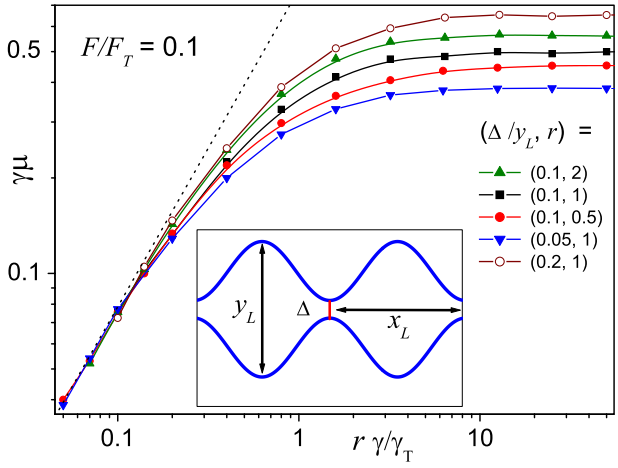

Fig. 1: (Color online) Rescaled mobility, $\gamma\mu$, *vs.* rescaled damping constant, $r\gamma/\gamma_T$, in the corrugated channel of eq. (2) at small drive, $F/F_T = 0.1$, and for different pore sizes, Δ/y_L, and aspect ratio, $r = x_L/y_L$. All quantities are expressed in dimensionless units with scaling parameters $r = x_L/y_L$, $F_T = kT/\Delta$ and $\gamma_T = \sqrt{mkT}/\Delta$, see eq. (3). The dotted line is the fitting law of eq. (5). The actual parameter values used in our simulations are $m = kT = y_L = 1$. Inset: corrugated channel with the boundary function $w(x)$ given in eq. (2).

action of the channel bottlenecks. Thus, the condition of vanishingly narrow pores, $\Delta \to 0$, assumed in most analytical studies, can be inconsistent with the assumption of overdamped diffusion in the spirit of the Smoluchowski approximation [18]. Finally, we also discuss applications to transport in colloidal systems.

Let us consider a point-like Brownian particle diffusing in a two-dimensional (2D) suspension fluid contained in a periodic channel with unit cell $x_L \times y_L$, as illustrated in fig. 1 (inset). The particle is subjected to a homogeneous force $\vec{F} = F\vec{e}_x$ oriented along the x-axis. The damped Brownian particle obeys the 2D Langevin equation

$$m\mathrm{d}^2\vec{r}/\mathrm{d}t^2 = -\gamma\ \mathrm{d}\vec{r}/\mathrm{d}t + \vec{F} + \sqrt{2\gamma kT}\ \vec{\xi}(t), \qquad (1)$$

where $\vec{r} = (x, y)$. The random forces $\vec{\xi}(t) = (\xi_x(t), \xi_y(t))$ are zero-mean, white Gaussian noises with autocorrelation functions $\langle \xi_i(t)\xi_j(t')\rangle = \delta_{ij}\delta(t-t')$, with $i, j = x, y$. The symmetric walls of the corrugated channel have been modeled by the sinusoidal function $\pm w(x)$ (fig. 1, inset),

$$w(x) = (1/4)[(y_L + \Delta) - (y_L - \Delta)\cos(2\pi x/x_L)]. \qquad (2)$$

With this choice for $w(x)$ we made explicit contact with the current literature on entropic channels [4–10]. However, similar results were obtained for sharper corrugation profiles, *e.g.*, for compartmentalized channels [13–16] (not reported here). We numerically integrated eq. (1) by a Milstein algorithm [19] with time step, Δt, ranging from 10^{-6} down to 10^{-9}, as F was increased. For each run, Δt was set small enough for the output to be independent of it. The stochastic averages reported below were obtained as ensemble averages over 10^6 trajectories with random initial conditions; transient effects were estimated and subtracted.

Two quantifiers have been used to characterize the Brownian transport in such sinusoidally corrugated channel:

i) Mobility. The response of a Brownian particle in a channel subjected to a dc drive, F, oriented along the x-axis, is expressed by the mobility, $\mu(F) = \langle v(F)\rangle/F$, where $\langle v\rangle \equiv \langle \dot{x}(F)\rangle = \lim_{t\to\infty}[\langle x(t)\rangle - x(0)]/t$. The function $\mu(F)$ increases from a relatively small value for $F = 0$, *i.e.*, $\mu(F=0) = \mu_0$, up to the free-particle limit, $\gamma\mu_\infty = 1$, for $F \to \infty$ [10]. We recall that in the bulk, a free particle drifts with speed F/γ.

ii) Diffusivity. As a Brownian particle is driven across a periodic array of bottlenecks or compartment pores, its diffusivity, $D(F) = \lim_{t\to\infty}[\langle x^2(t)\rangle - \langle x(t)\rangle^2]/2t$, picks up a distinct F-dependence. In corrugated channels with smooth bottlenecks, for $F \to \infty$ the function $D(F)$ approaches the free or bulk diffusion limit, $D(\infty) = D_0 \equiv kT/\gamma$, after going through an excess diffusion peak centered around an intermediate (temperature-dependent [10]) value of the drive. Such a peak signals the depinning of the particle from the barrier array of $w(x)$ associated with the channel bottlenecks [20].

Recall that, in the absence of external drives and for any value of the damping constant, Einstein's relation, $\gamma\mu_0 = D(F=0)/D_0$, establishes the dependence of the transport parameters on the temperature and the channel compartment geometry under equilibrium conditions.

Inertial effects in corrugated channels become apparent both for small γ and for large F. By inspecting figs. 1 and 2 we immediately realize that (for small γ) inertia tends to suppress the particle mobility through the channel bottlenecks. At large F, when plotted *vs.* γ (fig. 2(a)), the rescaled mobility approaches unity for $\gamma \to \infty$, as expected in the Smoluchowski approximation [10], but drops to zero in the underdamped limit, $\gamma \to 0$. More remarkably, the resulting $\gamma\mu$ curves shift to higher γ on increasing F (main panel). On expressing γ in units of $\gamma_F = \sqrt{mF/\Delta}$, see eq. (4) below, the curves for large drives tend to collapse on a universal curve well fitted by the power law $(\gamma/\gamma_F)^\alpha$ with $\alpha = 1.4$ (inset). Correspondingly, in fig. 2(b) the mobility grows like $\Delta^{\alpha/2}$ at large F (inset) and decays like $F^{-\alpha/2}$ for small Δ (main panel).

The power law, $\gamma\mu \propto (\gamma/\gamma_F)^\alpha$, introduced here is only a convenient fit of the rescaled mobility function, even if it holds for two or more decades of γ/γ_F. The analytical form of that function remains to be determined. Deviations from the fitted power law, $\mu \propto \Delta^{\alpha/2}$, for the mobility at very small Δ (fig. 2(b), inset), suggest that the fitting exponent, α, slightly depends on Δ, with $\alpha \to 2$ in the limit $\Delta \to 0$ (not shown). (Note that, on the contrary, the power law $\gamma\mu \propto F^{-\alpha/2}$ works throughout the entire F range explored in fig. 2(b).)

The dependence of the rescaled mobility on the system parameters in the underdamped limit is further illustrated

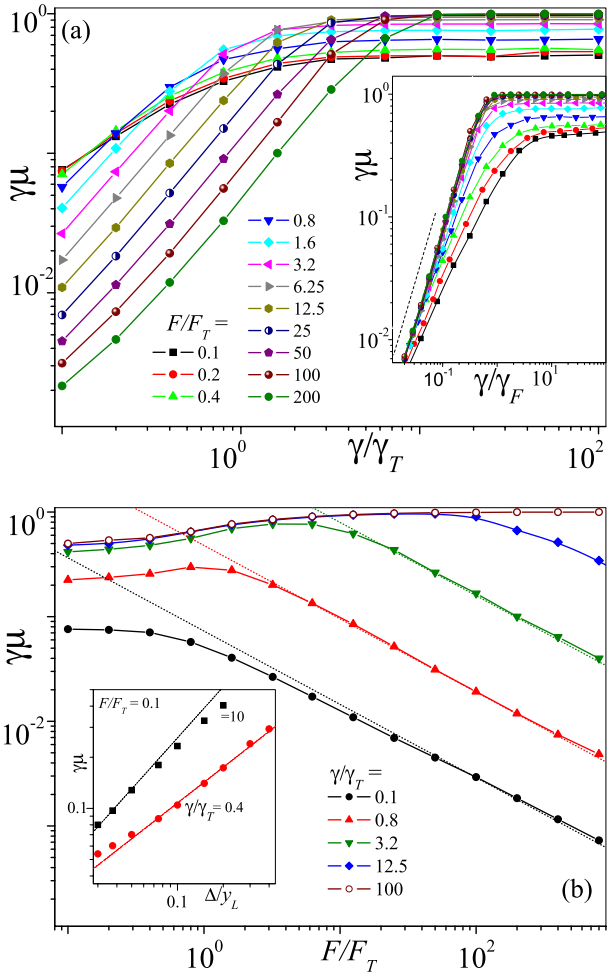

Fig. 2: (Color online) Rescaled mobility, $\gamma\mu$, in a corrugated channel with aspect ratio $r = 1$, rescaled pore size $\Delta/y_L = 0.1$, and (a) *vs.* the rescaled damping γ/γ_T for different force values F; (b) *vs.* F/F_T for various γ. The scaling parameters are $F_T = kT/\Delta$ and $\gamma_T = \sqrt{mkT}/\Delta$; the actual simulation parameters were set to $m = kT = y_L = 1$, as in fig. 1. Inset in (a): data from the main panel after different rescaling of damping constant, γ/γ_F, with $\gamma_F = \sqrt{mF/\Delta}$, see eq. (4); the raising branch of the universal curve for large drives is fitted by the power law $(\gamma/\gamma_F)^\alpha$ with $\alpha = 1.4$. Inset in (b): $\gamma\mu$ *vs.* Δ/y_L for $\gamma/\gamma_T = 0.4$ and two values of F. The dotted lines in (b) represent the large-drive power laws $(F/F_T)^{-\alpha/2}$ (main panel) and $(\Delta/y_L)^{\alpha/2}$ (inset), both with $\alpha = 1.4$; for $F/F_T = 1$, μ is proportional to Δ (inset).

in fig. 1, where at low γ and for vanishingly small drives, the mobility grows proportional to the aspect ratio $r = x_L/y_L$ of the channel unit cell and the pore cross-section Δ, *i.e.*, it scales with the dimensionless quantity $r\gamma/\gamma_T$ (see also the data set for $F/F_T = 1$ in the inset of fig. 2(b)).

Deviations of the diffusivity data from the expected overdamped behavior are even more prominent. As shown in fig. 3, at large γ the curves $D(F)$ approach the horizontal asymptote $D(F) = D_0$, as expected [10]. However, beyond a certain value of F, seemingly proportional to γ^2 (see figure inset), these curves abruptly depart from

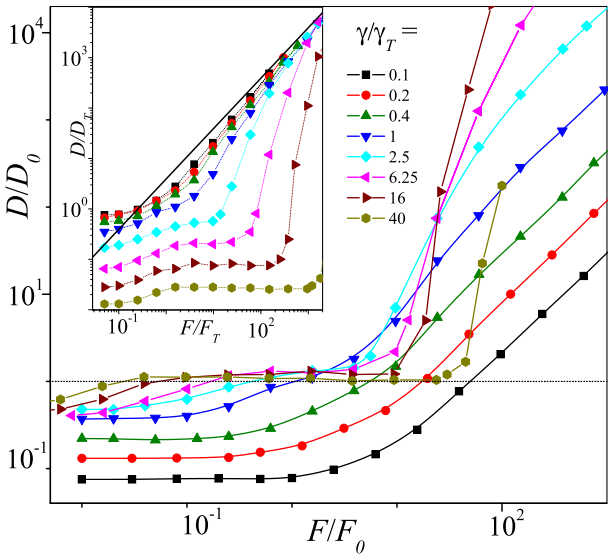

Fig. 3: (Color online) Rescaled diffusivity, D/D_0, *vs.* rescaled force, F/F_0, (main panel) and the rescaled diffusion coefficient D/D_T *vs.* F/F_T (inset) in the corrugated channel of eq. (2) with aspect ratio $r = 1$, rescaled pore width $\Delta/y_L = 0.1$, and different friction coefficients γ. The actual simulation parameters are $m = kT = y_L = 1$. The meaning of the scaling parameters, $D_T = kT/\gamma_T$, $F_0 = \gamma\sqrt{kT/m}$, and $F_T = kT/\Delta$, is discussed in the text. The solid line in the inset is the heuristic power law of eq. (6).

their horizontal asymptote. In the underdamped limit, the F-dependence of the diffusivity bears no resemblance with the typical overdamped behavior. At low γ, all $D(F)$ data sets collapse to a unique curve (fig. 3, inset), which tends to a value smaller than D_0 for $F \to 0$, and diverges for $F \to \infty$, like F^β with $\beta \simeq 1$. Such power law holds for large γ, as well, though in the large-F domain, only. Indeed, for exceedingly large F, all $D(F)$ curves seem to eventually approach a unique asymptote, irrespective of γ.

By comparing the plots of figs. 1–3 we conjecture that corrections due to inertia become significant in two regimes:

i) at *low drives* for

$$\gamma \lesssim \gamma_T = \sqrt{mkT}/\Delta. \tag{3}$$

This characteristic damping was used to rescale the mobility data in fig. 1 (see also fig. 2(b), inset); moreover, in fig. 3, for $\gamma < \gamma_T$ the diffusivity becomes a monotonic function of F with no plateau around D_0. The physical meaning of γ_T is simple. For $\gamma < \gamma_T$ the *thermal* length $l_T = \sqrt{mkT}/\gamma$ grows larger than the width of the pores, Δ, so that the Brownian particle cannot reach the normal diffusion regime, implicit in Einstein's relation, before bouncing off the pore walls. As a consequence, the Smoluchowski approximation fails in the vicinity of the bottlenecks.

Replacing γ with γ_T in the bulk quantities D_0 and F_0 yields, respectively, $D_T = kT/\gamma_T$ and $F_T = kT/\Delta$. These are the γ-independent rescaling factors introduced in

figs. 1–3 to characterize the inertia effects of the pore constrictions;

ii) at *high drives*, for

$$\gamma \lesssim \gamma_F = \sqrt{mF/\Delta}. \tag{4}$$

In the presence of a strong dc drive, the condition $\gamma \gg \gamma_T$ does not suffices to ensure normal diffusion; the additional condition $\Delta > l_F$ is required. Here, $l_F = mF/\gamma^2$ represents the *ballistic* length of a driven-damped particle, which is an estimate of the bouncing amplitude of a driven particle against the bottleneck. Upon increasing F at constant γ, l_F eventually grows larger than Δ and inertia comes into play for $\gamma_F \gtrsim \gamma$. This mechanism is clearly responsible for the abrupt increasing branches of $D(F)$ in fig. 3.

An analytical derivation of the transport quantifiers in the presence of strong inertial effects (low γ and/or large F) proved a difficult task. However, the following phenomenological arguments can explain our numerical findings.

Let us first consider the rescaled mobility at low drives. For $F = 0$ the transport quantifiers $\gamma\mu_0$ and $D(0)$ can be formally expressed in terms of the mean exit time, $\bar{\tau}_e$, of the Brownian particle out of a single compartment, namely, $D(0) = x_L^2/4\bar{\tau}_e$ and $\mu_0 = D(0)/kT$ (Einstein's relation). An analytical expression for $\bar{\tau}_e$ as a function of the compartment geometry is only available in the Smoluchowski approximation [17]. In the low-damping regime, we only have a rough estimate of $\bar{\tau}_e$. For $F = 0$ the particle bounces off a compartment wall with rate $(2/\pi)(2\sqrt{kT/m}/x_L)$ (attack frequency), but only a fraction Δ/y_L of such collisions leads to pore crossing. As a consequence, $\bar{\tau}_e \sim 4x_L y_L \sqrt{m/kT}/\pi\Delta$ and

$$\gamma\mu_0 \sim \frac{\pi}{4}\frac{\gamma x_L}{\sqrt{kT}}\frac{\Delta}{y_L} = \frac{\pi}{4}\left(r\frac{\gamma}{\gamma_T}\right), \tag{5}$$

which closely reproduces the numerical data of fig. 1 for $F/F_T = 1$ with mobility $\mu \propto \Delta$.

The divergence of the diffusivity with the drive shown in fig. 3, $D(F) \propto F^\beta$ with $\beta = 1$, is surprising since in the Smoluchowski approximation $D(F)$ always tends to its bulk value, D_0. A heuristic explanation for this asymptotic power law runs as follows. The dispersion of a strongly driven particle at low damping is due to its bouncing back and forth inside the channel cells with speed $\pm\bar{v}$ and $\bar{v} = F/\gamma$. Therefore, $D(F) = \bar{v}^2\bar{\tau}_e/4$, where $\bar{\tau}_e$ is the particle mean exit time through one of the pores of a channel cell, $\bar{\tau}_e = (\pi/2)(x_L/\bar{v})(\gamma/\gamma_T)$. The time constant $\bar{\tau}_e$ is estimated here as the cell crossing time, $x_L/\bar{v}$, multiplied by the geometric factor $\pi/2$ (also used to derive eq. (5)) and the success probability, γ/γ_T, for the particle to actually cross the bottleneck during a sequence of correlated bounces extending over the relaxation time m/γ. One thus concludes that $D(F) = (\pi/8)(x_L\Delta F)/\sqrt{mkT}$, or, in rescaled units of γ_T and D_T,

$$\frac{D(F)}{D_T} = \frac{\pi}{8}\frac{x_L F}{kT}, \tag{6}$$

in rather good agreement with our simulation data (see inset of fig. 3). Lowering the temperature, for small damping $D(F)$ diverges like $T^{-1/2}$, which means that diffusion is dominated by a (chaotic) mechanism of ballistic collisions.

The main result of this work is that for real physical suspensions flowing through compartmentalized geometries, both in biological and artificial systems, the limit of vanishingly small pore size becomes extremely sensitive to the finite viscosity of the suspension fluid. With respect to previous attempts at incorporating finite-mass effects in the analysis of Brownian transport through corrugated narrow channels [21], we stress that the inertial effects reported here are not of mere academic interest. Indeed, such effects can become appreciable even at low Reynolds numbers and for relatively small drives, where the viscous action of the fluid on a suspended particle is well described by Stokes' term in eq. (1) —*i.e.*, hydrodynamic corrections are negligible.

Inertial effects can be directly observed, for instance, in a dilute solution of colloidal particles driven across a porous membrane or an artificial sieve [22]. To be specific, let us consider spherical polystyrene beads [23] of radius $r_0 = 1\,\mu$m, suspended in a low viscous medium with, say, $\eta = 8.9 \times 10^{-4}\,\mathrm{Pa\cdot s}$ (water), $6.0 \times 10^{-4}\,\mathrm{Pa\cdot s}$ (benzene) or $3.6 \times 10^{-4}\,\mathrm{Pa\cdot s}$ (acetone). For the typical mass density of polystyrene, $200\,\mathrm{kg/m^3}$, the mass of a spherical bead of radius $r_0 = 1\,\mu$m is $m \simeq 8.4 \times 10^{-16}\,$kg. The corresponding rescaled damping constant γ/m, eq. (1), can be determined by making use of Stokes' law, $\gamma/m = 6\pi\eta r_0/m$, namely $\gamma/m \simeq 2.0 \times 10^{-5}\,\mathrm{ps^{-1}}$ (water), $1.4 \times 10^{-5}\,\mathrm{ps^{-1}}$ (benzene) and $8.1 \times 10^{-6}\,\mathrm{ps^{-1}}$ (acetone).

At room temperature, $T = 300\,$K, the thermal energy unit is $kT = 4.14 \times 10^{-21}\,\mathrm{kg\,m^2/s^2}$. If the pore radius is, say, 10% larger than r_0, then the effective width $\tilde{\Delta}$ for the finite-radius particle to go through the pore, becomes $\tilde{\Delta} = \Delta - 2r_0 = 0.2\,\mu$m and the rescaled zero-drive damping threshold $\gamma_T/m = \sqrt{kT/m\tilde{\Delta}^2}$ equals $1.1 \times 10^{-8}\,\mathrm{ps^{-1}}$. Here, $\gamma_T \ll \gamma$, which justifies the applicability of the overdamped dynamics. Nevertheless, for effective widths in the order of nanometers, *i.e.*, $\tilde{\Delta} = 0.002\,\mu$m, $\gamma_T/m \simeq 2.2 \times 10^{-6}\,\mathrm{ps^{-1}}$ reaches the order of the rescaled damping constant of acetone reported above.

Moreover, the corresponding non-scaled large-drive damping threshold $\gamma_F/m = \sqrt{F/m\tilde{\Delta}}$ can be easily achieved when applying dielectrophoretic forces. Depending on the size of the electrodes, dielectrophoretic forces acting on particles with radius $1\,\mu$m can result in pulling forces of up to 100 pN [24]. As a consequence, $\gamma_F/m \simeq 1.1 \times 10^{-5}\,\mathrm{ps^{-1}} > \gamma_F/m$. For suspended particles of even larger radius or higher mass density, both conditions $\gamma < \gamma_T$ and $\gamma < \gamma_F$ are also experimentally achievable.

In conclusion, the experimental demonstration of inertial effects on Brownian transport through narrow pores is accessible by manipulating artificial particles of moderate

size by means of well-established experimental techniques (see also [25]). For too small particles, like biological molecules, detecting such effects might require, however, more refined experimental setups.

* * *

This work was partly supported by the European Commission under grant No. 256959 (NANOPOWER) (FM), the Volkswagen foundation project I/83902 (PH, GS), the German excellence cluster "Nanosystems Initiative Munich" (NIM) (PH, GS), the Augsburg Center for Innovative Technology (ACIT) of the University of Augsburg (FM, PH), and the Japanese Society for Promotion of Science (JSPS) through Fellowship No. P11502 (PKG) and No. S11031 (FM). FN is partially supported by the ARO, NSF grant No. 0726909, JSPS-RFBR contract No. 12-02-92100, Grant-in-Aid for Scientific Research (S), MEXT Kakenhi on Quantum Cybernetics, and the JSPS via its FIRST program.

REFERENCES

[1] Hille B., *Ion Channels of Excitable Membranes* (Sinauer, Sunderland) 2001; Kärger J., *Diffusion in Zeolites and Other Microporous Solids* (Wiley, New York) 1992.
[2] Brenner H. and Edwards D. A., *Macrotransport Processes* (Butterworth-Heinemann, New York) 1993.
[3] Hänggi P. and Marchesoni F., *Rev. Mod. Phys.*, **81** (2009) 387.
[4] Burada P. S., Hänggi P., Marchesoni F., Schmid G. and Talkner P., *ChemPhysChem*, **10** (2009) 45.
[5] Zwanzig R., *J. Phys. Chem.*, **96** (1992) 3926.
[6] Reguera D. and Rubí J. M., *Phys. Rev. E*, **64** (2001) 061106.
[7] Kalinay P. and Percus J. K., *Phys. Rev. E*, **74** (2006) 041203.
[8] Laachi N., Kenward M., Yariv E. and Dorfman K. D., *EPL*, **80** (2007) 50009.
[9] Reguera D., Schmid G., Burada P. S., Rubí J. M., Reimann P. and Hänggi P., *Phys. Rev. Lett.*, **96** (2006) 130603.
[10] Burada P. S., Schmid G., Reguera D., Rubí J. M. and Hänggi P., *Phys. Rev. E*, **75** (2007) 051111.
[11] Reichelt R., Günther S., Wintterlin J., Moritz W., Aballe L. and Mentes T. O., *J. Phys. Chem.*, **127** (2007) 134706.
[12] Jacobs M. H., *Diffusion Processes* (Springer, New York) 1967.
[13] Marchesoni F. and Savel'ev S., *Phys. Rev. E*, **80** (2009) 011120; Ghosh P. K., Marchesoni F., Savel'ev S. and Nori F., *Phys. Rev. Lett.*, **104** (2010) 020601.
[14] Makhnovskii Yu. A., Berezhkovskii A. M. and Zitserman V. Yu., *J. Chem. Phys.*, **131** (2009) 104705.
[15] Borromeo M., Marchesoni F. and Ghosh P. K., *J. Chem. Phys.*, **134** (2011) 051101.
[16] Hänggi P., Marchesoni F., Savel'ev S. and Schmid G., *Phys. Rev. E*, **82** (2010) 041121.
[17] Schuss Z., Singer A. and Holcman D., *Proc. Natl. Acad. Sci. U.S.A.*, **104** (2007) 16098; Holcman D., Hoze N. and Schuss Z. D., *Phys. Rev. E*, **84** (2011) 021906; **85** (2012) 039903(E).
[18] Tikhonov V. I., *Avtom. Telemekh.*, **21** (1960) 301; Wilemski G., *J. Stat. Phys.*, **14** (1976) 153; Titulaer U. M., *Physica A*, **91** (1978) 321; Skinner J. L. and Wolynes P., *Physica A*, **96** (1979) 561.
[19] Kloeden P., *Numerical Solutions of Stochastic Differential Equations* (Springer, Berlin) 1999.
[20] Costantini G. and Marchesoni F., *Europhys. Lett.*, **48** (1999) 491.
[21] Berezhkovskii A. M. and Szabo A., *J. Chem. Phys.*, **135** (2011) 074108; Martens S., Sokolov I. M. and Schimansky-Geier L., *J. Chem. Phys.*, **136** (2012) 111102; Kalinay P. and Percus J., arXiv:1204.1145v1 (2012).
[22] Mark J. E., *Polymer Data Handbook* (Oxford University Press, New York) 1999.
[23] Garbow N., Evers M., Palberg T. and Okubo T., *J. Phys.: Condens. Matter*, **16** (2004) 3835.
[24] Morgan H. and Green N. G., *AC Electrokinetics: Colloids and Nanoparticles* (Research Studies Press LTD., Baldock, Hertfordshire, England) 2003.
[25] Li T., Kheifets S., Medellin D. and Raizen M., *Science*, **328** (2010) 1673; Huang R., Chavez I., Taute K., Lukic B., Jeney S., Raizen M. and Florin E., *Nat. Phys.*, **7** (2011) 576; Franosch T., Grimm M., Belushkin M., Mor F., Foffi G., Forró L. and Jeney S., *Nature*, **478** (2011) 85; Jannasch A., Mahamdeh M. and Schäffer E., *Phys. Rev. Lett.*, **107** (2011) 228301.